Published as: *Nat Med*. 2008 April ; 14(4): 442–447.

Genetic and pharmacologic inhibition of mitochondrial-dependent necrosis attenuates muscular dystrophy

Douglas P Millay[1,2], **Michelle A Sargent**[1], **Hanna Osinska**[1], **Christopher P Baines**[1], **Elisabeth R Barton**[3], **Grégoire Vuagniaux**[4], **H Lee Sweeney**[5], **Jeffrey Robbins**[1], and **Jeffery D Molkentin**[1]

[1] *Department of Pediatrics, University of Cincinnati, Cincinnati Children's Hospital Medical Center, 3333 Burnet Avenue, Cincinnati, Ohio 45229, USA* [2] *Department of Molecular Genetics, Biochemistry and Microbiology, University of Cincinnati, 231 Albert Sabin Way, Cincinnati, Ohio 45267, USA* [3] *Department of Anatomy and Cell Biology, University of Pennsylvania School of Dental Medicine, 240 South 40th Street, Philadelphia, Pennsylvania 19104, USA* [4] *DebioPharm S.A., Chemin Messidor 5–7, 1002 Lausanne, Switzerland* [5] *Department of Physiology, University of Pennsylvania School of Medicine, 3700 Hamilton Walk, Philadelphia, Pennsylvania 19104, USA*

Abstract

Muscular dystrophies comprise a diverse group of genetic disorders that lead to muscle wasting and, in many instances, premature death[1]. Many mutations that cause muscular dystrophy compromise the support network that connects myofilament proteins within the cell to the basal lamina outside the cell, rendering the sarcolemma more permeable or leaky. Here we show that deletion of the gene encoding cyclophilin D (*Ppif*) rendered mitochondria largely insensitive to the calcium overload–induced swelling associated with a defective sarcolemma, thus reducing myofiber necrosis in two distinct models of muscular dystrophy. Mice lacking δ-sarcoglycan (*Scgd*$^{-/-}$ mice) showed markedly less dystrophic disease in both skeletal muscle and heart in the absence of *Ppif*. Moreover, the premature lethality associated with deletion of *Lama2*, encoding the α-2 chain of laminin-2, was rescued, as were other indices of dystrophic disease. Treatment with the cyclophilin inhibitor Debio-025 similarly reduced mitochondrial swelling and necrotic disease manifestations in *mdx* mice, a model of Duchenne muscular dystrophy, and in *Scgd*$^{-/-}$ mice. Thus, mitochondrial-dependent necrosis represents a prominent disease mechanism in muscular dystrophy, suggesting that inhibition of cyclophilin D could provide a new pharmacologic treatment strategy for these diseases.

The muscular dystrophies are inherited disorders that mostly affect striated muscle tissue, resulting in progressive muscle weakness, wasting and, in many instances, premature death[1]. Many characterized mutations in humans that result in muscular dystrophy cause alterations either in structural proteins that attach the underlying contractile proteins to the basal lamina, which provides rigidity to the skeletal muscle cell membrane (sarcolemma), or in proteins that

Correspondence should be addressed to J.D.M. (jeff.molkentin@cchmc.org).

AUTHOR CONTRIBUTIONS

D.P.M. performed most of the experiments with technical help from M.A.S., C.P.B. and H.O. E.R.B. performed the force measurements in EDL within the Wellstone center grant to H.L.S. G.V. consulted on studies with Debio-025 and provided the compound. J.R. provided support through the use of electron microscopy. J.D.M. planned and supervised all experimentation.

COMPETING INTERESTS STATEMENT

The authors declare competing financial interests: details accompany the full-text HTML version of the paper at http://www.nature.com/naturemedicine/.

directly stabilize or repair the cell membrane[1–3]. For example, loss of dystrophin or other components of the dystrophin-glycoprotein complex leads to a fundamental alteration in the physical properties of the sarcolemma, permitting contraction-induced microtears and the unregulated exchange of ions, increasing the influx of calcium[2–4]. Moreover, total intracellular calcium or subsarcolemmal calcium levels have been found to be elevated in skeletal muscle cells or fibers from dystrophic mice[5,6].

In response to sustained increases in intracellular calcium concentrations, such as after ischemic injury, mitochondria undergo a so-called 'permeability transition'[7]. This process results in the regulated formation of a large pore complex that spans the outer and inner mitochondrial membranes, leading to an irreversible loss of matrix and intermembrane contents and swelling of the mitochondria. If this transition state is not reversed in a timely manner, the mitochondria can rupture, causing necrotic and/or apoptotic cell death. Cyclophilin D is a mitochondrial matrix prolyl *cis-trans* isomerase that directly regulates calcium- and reactive oxygen species–dependent mitochon-drial permeability transition (MPT) and cellular necrosis. Indeed, mice lacking *Ppif* show protection from necrotic cell death in the brain and heart after ischemic injury, and mitochondria isolated from these mice are resistant to calcium-induced swelling[8–11].

Given that many of the pathologic features leading to MPT are present in muscular dystrophy, we first analyzed this potential association in *Scgd*$^{-/-}$ mice, a model of severe dystrophy in both skeletal muscle and heart. Mitochondria isolated from dystrophic skeletal muscle of *Scgd*$^{-/-}$ mice were swollen compared to those from wild-type mice, but deletion of *Ppif* largely prevented this phenotype (Fig. 1a). Mitochondria isolated from *Scgd*$^{-/-}$ skeletal muscle were also refractory to additional swelling induced by exogenously applied calcium (200 μM), given their already swollen state, and they showed more shrinkage in response to a hyperosmotic shock induced by polyethylene glycol (PEG; data not shown). *Scgd*$^{-/-}$ mice initially showed a pseudohypertrophy response (an initial increase in total muscle weight due to inflammation and regeneration, but not associated with increased muscle mass *per se*) at 6 weeks of age owing to tissue inflammation and ongoing degeneration of myofibers (Fig. 1b). However, in both the gastrocnemius and the quadriceps, this process was blocked in *Scgd*$^{-/-}$ mice that also lacked the *Ppif* gene, and *Ppif* single null mutant mice were normal (Fig. 1b). By 8 months of age, *Scgd*$^{-/-}$ mice showed a profound reduction in muscle weight owing to severe degeneration, but deletion of the *Ppif* gene prevented this process and maintained normal muscle weights (Fig. 1c). Thus, deletion of the *Ppif* gene mitigates the mitochondrial swelling associated with muscular dystrophy and the secondary alterations in muscle weight as the disease progresses.

To more carefully analyze the phenotype of *Scgd*$^{-/-}$*Ppif* $^{-/-}$ mice, we performed a series of histological and biochemical assays. Diaphragm and gastrocnemius muscle from *Scgd*$^{-/-}$ mice showed the characteristic increase in central nucleation of myofibers that indicates regeneration due to ongoing degeneration, and this regeneration was significantly reduced in *Scgd*$^{-/-}$*Ppif* $^{-/-}$ mice (Fig. 1d and data not shown). Diaphragm and gastrocnemius muscle from *Scgd*$^{-/-}$*Ppif* $^{-/-}$ mice also showed a more uniform profile of myofiber areas, fewer smaller fibers and a greater number of larger fibers compared with muscle from *Scgd*$^{-/-}$ mice (Fig. 1e and data not shown). Finally, *Scgd*$^{-/-}$*Ppif* $^{-/-}$ mice showed a significant decrease in total fiber number within the gastrocnemius compared with *Scgd*$^{-/-}$ mice, further suggesting less ongoing degeneration-regeneration (Fig. 1f). Gross histological examination of the diaphragm, gastrocnemius and quadriceps also revealed a reduction in pathology in *Scgd*$^{-/-}$*Ppif* $^{-/-}$ mice compared with *Scgd*$^{-/-}$ mice (Fig. 1g). Direct measurement of muscle force generation from the isolated extensor digitorum longus (EDL) from *Scgd*$^{-/-}$ mice showed a significant reduction in specific force that was restored by deletion of *Ppif* (Fig. 1h). However, the deletion of *Ppif* did not produce a functional recovery in diaphragm specific force generation in the absence of *Scgd*, suggesting some heterogeneity in the functional improvement (data not shown).

Degeneration of myofibers leads to the recruitment of inflammatory cells. Skeletal muscle from *Scgd*$^{-/-}$*Ppif*$^{-/-}$ mice showed less T cell invasion and fewer inflammatory cells (and less inflammatory cell activity) at 6 weeks and 6 months of age compared with *Scgd*$^{-/-}$ mice, further suggesting a reduction in myofiber degeneration in the absence of cyclophilin D (Supplementary Fig. 1 online). However, direct biochemical assessment of tissue fibrosis using a hydroxyproline assay showed no reduction in fibrosis in *Scgd*$^{-/-}$*Ppif*$^{-/-}$ mice compared with *Scgd*$^{-/-}$ mice at 8 months of age, although a trend toward a reduction was observed at 6 weeks of age (Supplementary Fig. 1). These results support the overall conclusion that inhibition of MPT through deletion of *Ppif* protects dystrophic skeletal muscle by reducing myofiber degeneration. Direct examination of this hypothesis by electron microscopy showed areas of extensive myofiber necrosis and swollen mitochondria in the gastrocnemius, diaphragm and EDL of *Scgd*$^{-/-}$ mice; this pathology was markedly reduced in *Scgd*$^{-/-}$*Ppif*$^{-/-}$ mice (Fig. 2a, Supplementary Fig. 2 online and data not shown). To more directly quantify myofiber necrosis, we used an assay in which *in situ* ligation of a hairpin probe detects DNA strand breaks that correspond to necrotic events[12]. Use of this assay in *Scgd*$^{-/-}$ gastrocnemius histological sections revealed a 2% frequency of necrotic nuclei compared with none observed in wild-type muscle, whereas *Scgd*$^{-/-}$*Ppif*$^{-/-}$ mice showed a significantly lower frequency of about 0.5% (Fig. 2b).

Fragile sarcolemmas in mouse models of muscular dystrophy can be directly visualized by leakage of Evan's blue dye (EBD) into myofibers after systemic injection of the dye. Whereas wild-type mice showed no EBD uptake in the gastrocnemius or quadriceps after voluntary wheel running, both *Scgd*$^{-/-}$ and *Scgd*$^{-/-}$*Ppif*$^{-/-}$ mice showed similar numbers of dye-positive fibers, indicating that loss of *Ppif* was not able to stabilize the muscle fiber sarcolemma to prevent dye uptake (Fig. 2c,d). Consistent with the cardiac pathology seen in many forms of muscular dystrophy in humans, by 8 months of age *Scgd*$^{-/-}$ mice showed cardiac pathology characterized by a significant increase in tissue fibrosis and a reduction in function as measured by echocardiography (Fig. 2e–g). However, *Scgd*$^{-/-}$*Ppif*$^{-/-}$ mice had a significant reduction in cardiac fibrosis as assessed in histological sections (Fig. 2e) or by biochemical measurement of hydroxyproline content (Fig. 2f) compared with *Scgd*$^{-/-}$ mice. *Scgd*$^{-/-}$*Ppif*$^{-/-}$ mice also maintained cardiac function better than *Scgd*$^{-/-}$ mice at 8 months of age (Fig. 2g).

We also selected the *Lama2*$^{-/-}$ mouse for analysis given its more severe dystrophic phenotype compared to *Scgd*$^{-/-}$ mice and its uniform profile of premature lethality by 2 months of age. *Lama2*$^{-/-}$ mice also have neuronal defects that contribute to the extent of disease and their early lethality[13]. Mitochondria isolated from skeletal muscle of *Lama2*$^{-/-}$ mice at 3 weeks of age were noticeably swollen; however, this phenotype was almost completely reversed in mitochondria from *Lama2*$^{-/-}$*Ppif*$^{-/-}$ skeletal muscle (Fig. 3a). Notably, *Lama2*$^{-/-}$*Ppif*$^{-/-}$ mice had substantially enhanced survival, such that approximately 75% lived past 150 d, whereas all *Lama2*$^{-/-}$ mice died by 50 d of age (Fig. 3b). There was also a significant prolongation of life span (twofold) in *Lama2*$^{-/-}$ *Ppif*$^{+/-}$mice (Fig. 3b), which may be due to the slightly reduced sensitivity of their mitochondria to calcium overload[8]. In association with their increased survival, *Lama2*$^{-/-}$*Ppif*$^{-/-}$ mice showed more ambulation compared with *Lama2*$^{-/-}$ mice at 4 weeks of age and a larger increase in body weight during neonatal development (Fig. 3c and data not shown). At 3 weeks of age, the weights of various skeletal muscles from *Lama2*$^{-/-}$ mice were reduced compared with those from wild-type littermates; skeletal muscles from *Lama2*$^{-/-}$*Ppif*$^{-/-}$ mice had intermediate weights, indicating partial rescue of this defect (Fig. 3d). The decrease in total fiber number and mean fiber area in the gastrocnemius of *Lama2*$^{-/-}$mice was also significantly reversed in *Lama2*$^{-/-}$*Ppif*$^{-/-}$ mice, suggesting less ongoing degeneration-regeneration (Fig. 3e,f). Additionally, diaphragm and gastrocnemius muscle from *Lama2*$^{-/-}$ mice showed more fibrotic content than did these muscles from wild-type mice, and the fibrotic content was decreased by deletion of the *Ppif* gene (Fig. 3g). *Lama2*$^{-/-}$ mice had a significant increase in skeletal muscle myeloperoxidase activity (an

indicator of inflammation) compared with wild-type mice, and this phenotype was also rescued in *Lama2*$^{-/-}$*Ppif* $^{-/-}$ mice (Fig. 3h). Taken together, these results indicate that the effects of *Ppif* deficiency in *Lama2*$^{-/-}$ mice are nearly identical to those in *Scgd*$^{-/-}$ mice.

To translate our results observed in mice with a genetic deficiency of cyclophilin D into a potential treatment for muscular dystrophy, we investigated the ability of the cyclophilin inhibitor Debio-025 to reduce disease in both *Scgd*$^{-/-}$ mice and the *mdx* mouse model of Duchenne muscular dystrophy. Although Debio-025 seems to inhibit equally most cyclophilin family members, one of its more prominent effects is inhibition of cyclophilin D and MPT. *Mdx* mice were treated with Debio-025 at 50 mg/kg/d (injected subcutaneously) beginning at 4 weeks of age until 10 weeks of age. Mitochondria isolated from skeletal muscle of vehicle-treated *mdx* mice showed significant swelling that was reduced in Debio-025–treated *mdx* mice (Fig. 4a). Debio-025 treatment also prevented the pseudohypertrophy response in various skeletal muscles from *mdx* mice compared with vehicle-treated *mdx* mice, whereas C57BL/10 controls were unaffected by Debio-025 (Fig. 4b). Gross histologic examination of the diaphragm, gastrocnemius and quadriceps showed a noticeable improvement in myofiber organization and a reduction in fibrosis after Debio-025 treatment of *mdx* mice (Fig. 4c and Supplementary Fig. 3 online). Indeed, quantification of fibrosis in the diaphragm, tibialis anterior, gastrocnemius and quadriceps showed a significant reduction in fibrosis in Debio-025–treated versus vehicle-treated *mdx* mice (Fig. 4d). Central nucleation was also significantly reduced (Fig. 4e), and fiber area distributions were largely normalized after Debio-025 treatment of *mdx* mice (Supplementary Fig. 4 online).

Mice lacking *Scgd* were also treated with Debio-025 beginning at 4 weeks of age and ending at 10 weeks of age (50 mg/kg/d), resulting in a similar decrease in muscle pathology as observed in treated *mdx* mice (Supplementary Fig. 5 online). Debio-025 also reduced the cardiac hypertrophy associated with *Scgd* deletion (Supplementary Fig. 5). Additionally, Debio-025 partially normalized the fiber area distributions in *Scgd*$^{-/-}$ mice compared with vehicle-treated controls, further suggesting that cyclophilin D inhibition reduces degeneration-regeneration cycling (Supplementary Fig. 6 online).

We suggest a model in which sarcolemmal defects, resulting in altered calcium handling within the muscle cell, initiate muscular dystrophy in part through the triggering of MPT (Supplementary Fig. 7 online). The MPT pore is thought to consist of the voltage-dependent anion channel in the outer mitochondrial membrane, the adenine nucleotide translocase in the inner mitochondrial membrane and cyclophilin D in the matrix[7]. Loss of the *Ppif* gene profoundly affects the function of the MPT pore and its response to calcium overload and reactive oxygen species stimulation, leading to a dramatic attenuation of mitochondrial swelling and subsequent necrotic cell death[8–11]. One well-known pharmacologic inhibitor of cyclophilin D and the MPT process is cyclosporine. However, the use of cyclosporine is highly problematic because it also inhibits calcineurin, a signaling protein crucially involved in skeletal muscle regeneration after injury and in the differentiation of skeletal muscle cells[14,15]. Indeed, inhibition of calcineurin has been shown to worsen muscular dystrophy in the *mdx* mouse, whereas an activated transgene for calcineurin protected *mdx* mice[14,16,17]. Debio-025 is a more potent prolyl isomerase inhibitor than cyclosporine, is nonimmunosuppressive and does not block calcineurin activity, blocks cell death effectively in a number of contexts, and has shown efficacy against hepatitis C virus in human clinical trials[18–20].

Necrosis may have a central role in mediating myocyte and myofiber loss from the heart and skeletal muscle in response to various disease states associated with calcium dysregulation. For example, we have shown that calcium overload–induced necrosis of myocytes from the heart and associated cardiac dysfunction are reduced by *Ppif* gene deletion[21]. Similarly,

myopathy associated with collagen VI deficiency causes defects in mitochondrial architecture and function, calcium dysregulation, muscle ultrastructural defects and cell death that are partially rescued by administration of cyclo-sporine[22]. Cyclosporine and Debio-025 were also shown to reduce death of primary human myoblasts from collagen VI–deficient individuals in culture, as well as loss of mitochondrial membrane potential, following oligomycin and cyanide treatment[23]. Deletion of *Ppif* may also be efficacious in other disorders. Indeed, *Ppif* $^{-/-}$ mice showed less disease associated with experimental autoimmune encephalomyelitis, an animal model of multiple sclerosis[24]. Thus, mitochondrial-dependent necrosis may function as a common disease mechanism underlying many long-term degenerative disorders. In particular, our results suggest that inhibiting cyclophilin D may serve as a new approach for treating muscular dystrophies associated with a defective membrane by preventing or attenuating calcium-dependent necrosis through a mitochondrial-dependent pathway.

METHODS

Mice

Scgd$^{-/-}$ mice were generously provided by E. McNally and were described previously[25]. *Ppif* $^{-/-}$ mice were described previously[8], as were the *Lama2*$^{-/-}$ mutant mice[13]. We obtained *mdx* (C57BL/10) and control mice (C57BL/10) from Jackson Laboratories. We treated *Scgd*$^{-/-}$ and *mdx* mice with Debio-025 (in a cremaphor-based vehicle; DebioPharm) beginning at 4 weeks of age. Debio-025 was administered at 50 mg/kg/d and was delivered using 2 subcutaneous injections 12 h apart every day for 6 weeks. All mouse experimentation was approved by the Institutional Animal Care and Use Committee at Cincinnati Children's Hospital. We used both male and female mice.

Mitochondrial isolation and swelling assays

We performed mitochondrial isolation essentially as described previously[26]. We measured the light scattering of 250 μg of mitochondria in a 1-ml volume at 540 nm. We induced mitochondrial swelling or shrinkage by incubating mitochondria with 200 μM $CaCl_2$ or 5% PEG-3350 (wt/vol), respectively, for 10 min and measured absorbance at 540 nm every 10 s. Swelling and shrinkage were monitored as a reduction and an increase in absorbance, respectively.

Pathologic indices

We cut paraffin-embedded sections (7 μm thick) at the center of the muscle and stained them with wheat germ agglutinin conjugated to tetramethylrhodamine isothiocyanate (Sigma) for 1 h at room temperature, followed by nuclear staining with bis-benzamide (Sigma). We counted the number of fibers comprising the gastrocnemius at the mid-belly for each mouse. We counted approximately 600 fibers per mouse for each muscle group for analysis of central nucleation with ImageJ software[27]. We performed Masson's trichrome and H&E staining on paraffin-embedded sections.

Western blot analysis

We prepared protein extracts from the quadriceps by homogenization in cell lysis buffer (20 mM Tris (pH 7.4), 137 mM NaCl, 25 mM β-glycerophosphate, 2 mM sodium pyrophosphate, 2 mM EDTA, 1 mM sodium orthovanadate, 1% Triton X-100, 10% glycerol, 1 mM phenylmethanesulphonylfluoride, 5 μg/ml leupeptin, 5 μg/ml aprotinin and 2 mM benzamide). We then centrifuged extracts at 13,000*g* for 10 min. We separated 100 μg of supernatant on a SDS–12% polyacrylamide gel, transferred the proteins to a polyvinylidene difluoride membrane and immunodetected as specified by the manufacturer (Amersham Biosciences). We used antibodies to CD3 (Santa Cruz, 1:1,000 dilution) and GAPDH (Fitzgerald Industries,

1:2,500 dilution) for immunodetection, which we quantified on a Storm860 PhosphorImager (Molecular Dynamics).

Evaluation of hydroxyproline and myeloperoxidase content

We measured the hydroxyproline content in tissue as described previously[27]. Measurement of myeloperoxidase activity, as a surrogate for infiltration of neutrophils and macrophages, was also described previously[28].

Evan's blue dye uptake

We injected EBD (10 mg/ml in PBS) intraperitoneally (0.1 ml per 10 g body weight) and gave the mice access to exercise wheels overnight (all mice underwent similar amounts of wheel running). We killed the mice in the morning (approximately 18 h after injection). We dissected gastrocnemius and quadriceps muscles and embedded them in optimal cutting temperature compound (Tissue-Tek) and then snap-froze them in liquid nitrogen. We cut sections at a thickness of 7 μm, washed them briefly in PBS and stained them with wheat germ agglutinin conjugated to FITC for 1 h at room temperature. We took pictures at 100× magnification on a fluorescent microscope. EBD is detected as red auto-fluorescence.

Electron microscopy

We analyzed the gastrocnemius, diaphragm and EDL from wild-type, *Scgd*$^{-/-}$, and *Scgd*$^{-/-}$*Ppif*$^{-/-}$ mice (n = 2 for each group) for ultrastructural alterations as described previously[29].

Echocardiography

We anesthetized 8-month-old mice with 2% isoflurane and visualized their hearts with a Hewlett Packard Sonos 5500 ultrasound instrument and a 15-MHz transducer for echocardiography in the mouse. We measured cardiac ventricular dimensions using M-mode, and we performed this measurement three times for each mouse.

Muscle functional assessment

We extracted EDL and diaphragm muscles from wild-type, *Scgd*$^{-/-}$, *Scgd*$^{-/-}$*Ppif*$^{-/-}$, and *Ppif*$^{-/-}$ mice (n = 6 for each group, with 11–12 muscles analyzed) and measured the maximal tetanic force normalized to area as described previously[30].

Statistical analyses

The results are presented as means ± s.e.m. In cases where means of two independent groups were compared, we used a two-sample Student's t-test. We used a one-way ANOVA to compare means among 3 or more independent groups. We applied a Newman-Keuls *post-hoc* test using InStat 3.0 (GraphPad) whenever we conducted multiple comparisons. We used a two-way ANOVA for comparison of groups in the Debio-025 studies with the Newman-Keuls *post-hoc* test. For the survival curve, we performed a χ^2 test using Prism 3.0 software (GraphPad). We considered values as significant when $P < 0.05$.

Supplementary Material

Refer to Web version on PubMed Central for supplementary material.

Acknowledgements

This work was supported by grants from the National Institutes of Health (J.D.M., J.R.), an award from the Jain Foundation (J.D.M.), the Fondation Leducq (J.D.M.) and The Paul Wellstone Muscular Dystrophy Cooperative

Research Center of the National Institutes of Health (U54 AR052646 to H.L.S. and E.R.B.). D.P.M. was supported by National Institutes of Health training grant 5 T32 HL07382 (principal investigator A. Schwartz). We would like to thank X. Xiao at the University of Pittsburgh for supplying the *Lama2*$^{-/-}$ mice under permission from E. Engvall at the Burnham Institute. We would also like to thank E. McNally (University of Chicago) for the *Scgd*$^{-/-}$ mice.

References

1. Durbeej M, Campbell KP. Muscular dystrophies involving the dystrophin-glycoprotein complex: an overview of current mouse models. Curr Opin Genet Dev 2002;12:349–361. [PubMed: 12076680]
2. Lapidos KA, Kakkar R, McNally EM. The dystrophin glycoprotein complex: signaling strength and integrity for the sarcolemma. Circ Res 2004;94:1023–1031. [PubMed: 15117830]
3. Bansal D, et al. Defective membrane repair in dysferlin-deficient muscular dystrophy. Nature 2003;423:168–172. [PubMed: 12736685]
4. Whitehead NP, Yeung EW, Allen DG. Muscle damage in *mdx* (dystrophic) mice: role of calcium and reactive oxygen species. Clin Exp Pharmacol Physiol 2006;33:657–662. [PubMed: 16789936]
5. Turner PR, Westwood T, Regen CM, Steinhardt RA. Increased protein degradation results from elevated free calcium levels found in muscle from *mdx* mice. Nature 1988;335:735–738. [PubMed: 3173492]
6. Mallouk N, Jacquemond V, Allard B. Elevated subsarcolemmal Ca^{2+} in *mdx* mouse skeletal muscle fibers detected with Ca^{2+}-activated K. channels Proc Natl Acad Sci USA 2000;97:4950–4955.
7. Zamzami N, Kroemer G. The mitochondrion in apoptosis: how Pandora's box opens. Nat Rev Mol Cell Biol 2001;2:67–71. [PubMed: 11413468]
8. Baines CP, et al. Loss of cyclophilin D reveals a critical role for mitochondrial permeability transition in cell death. Nature 2005;434:658–662. [PubMed: 15800627]
9. Nakagawa T, et al. Cyclophilin D–dependent mitochondrial permeability transition regulates some necrotic but not apoptotic cell death. Nature 2005;434:652–658. [PubMed: 15800626]
10. Basso E, et al. Properties of the permeability transition pore in mitochondria devoid of cyclophilin D. J Biol Chem 2005;280:18558–18561. [PubMed: 15792954]
11. Schinzel AC, et al. Cyclophilin D is a component of mitochondrial permeability transition and mediates neuronal cell death after focal cerebral ischemia. Proc Natl Acad Sci USA 2005;102:12005–12010. [PubMed: 16103352]
12. Li B, et al. Insulin-like growth factor-1 attenuates the detrimental impact of nonocclusive coronary artery constriction on the heart. Circ Res 1999;84:1007–1019. [PubMed: 10325238]
13. Kuang W, et al. Merosin-deficient congenital muscular dystrophy. Partial genetic correction in two mouse models. J Clin Invest 1998;102:844–852. [PubMed: 9710454]
14. Stupka N, Gregorevic P, Plant DR, Lynch GS. The calcineurin signal transduction pathway is essential for successful muscle regeneration in *mdx* dystrophic mice. Acta Neuropathol 2004;107:299–310. [PubMed: 14727129]
15. Friday BB, Horsley V, Pavlath GK. Calcineurin activity is required for the initiation of skeletal muscle differentiation. J Cell Biol 2000;149:657–666. [PubMed: 10791979]
16. Chakkalakal JV, et al. Stimulation of calcineurin signaling attenuates the dystrophic pathology in *mdx* mice. Hum Mol Genet 2004;13:379–388. [PubMed: 14681302]
17. Stupka N, et al. Activated calcineurin ameliorates contraction-induced injury to skeletal muscles of *mdx* dystrophic mice. J Physiol (Lond) 2006;575:645–656. [PubMed: 16793906]
18. Hansson MJ, et al. The nonimmunosuppressive cyclosporin analogs NIM811 and UNIL025 display nanomolar potencies on permeability transition in brain-derived mitochondria. J Bioenerg Biomembr 2004;36:407–413. [PubMed: 15377880]
19. Flisiak R, et al. The cyclophilin inhibitor Debio-025 had a potent dual anti-HIV and anti-HCV activity in treatment-naive HIV/HCV co-infected subjects. Hepatology 2006;44(Suppl 1):609A.
20. Khaspekov L, Friberg H, Halestrap A, Viktorov I, Wieloch T. Cyclosporin A and its nonimmunosuppressive analogue *N*-Me-Val-4–cyclosporin A mitigate glucose/oxygen deprivation–induced damage to rat cultured hippocampal neurons. Eur J Neurosci 1999;11:3194–3198. [PubMed: 10510183]

21. Nakayama H, et al. Ca^{2+}- and mitochondrial-dependent cardiomyocyte necrosis as a primary mediator of heart failure. J Clin Invest 2007;117:2431–2444. [PubMed: 17694179]
22. Irwin WA, et al. Mitochondrial dysfunction and apoptosis in myopathic mice with collagen VI deficiency. Nat Genet 2003;35:367–371. [PubMed: 14625552]
23. Angelin A, et al. Mitochondrial dysfunction in the pathogenesis of Ullrich congenital muscular dystrophy and prospective therapy with cyclosporins. Proc Natl Acad Sci USA 2007;104:991–996. [PubMed: 17215366]
24. Forte M, et al. Cyclophilin D inactivation protects axons in experimental autoimmune encephalomyelitis, an animal model of multiple sclerosis. Proc Natl Acad Sci USA 2007;104:7558–7563. [PubMed: 17463082]
25. Hack AA, et al. Differential requirement for individual sarcoglycans and dystrophin in the assembly and function of the dystrophin-glycoprotein complex. J Cell Sci 2000;113:2535–2544. [PubMed: 10862711]
26. Fontaine E, et al. Regulation of the permeability transition pore in skeletal muscle mitochondria. Modulation by electron flow through the respiratory chain complex I. J Biol Chem 1998;273:12662–12668. [PubMed: 9575229]
27. Parsons SA, Millay DP, Sargent MA, McNally EM, Molkentin JD. Age-dependent effect of myostatin blockade on disease severity in a murine model of limb-girdle muscular dystrophy. Am J Pathol 2006;168:1975–1985. [PubMed: 16723712]
28. Suzuki K, et al. Overexpression of interleukin-1 receptor antagonist provides cardio-protection against ischemia-reperfusion injury associated with reduction in apoptosis. Circulation 2001;104:I308–I313. [PubMed: 11568074]
29. Fewell JG, et al. A treadmill exercise regimen for identifying cardiovascular phenotypes in transgenic mice. Am J Physiol 1997;273:H1595–H1605. [PubMed: 9321854]
30. Barton-Davis ER, et al. Viral-mediated expression of insulin-like growth factor I blocks the aging-related loss of skeletal muscle function. Proc Natl Acad Sci USA 1998;95:15603–15607. [PubMed: 9861016]

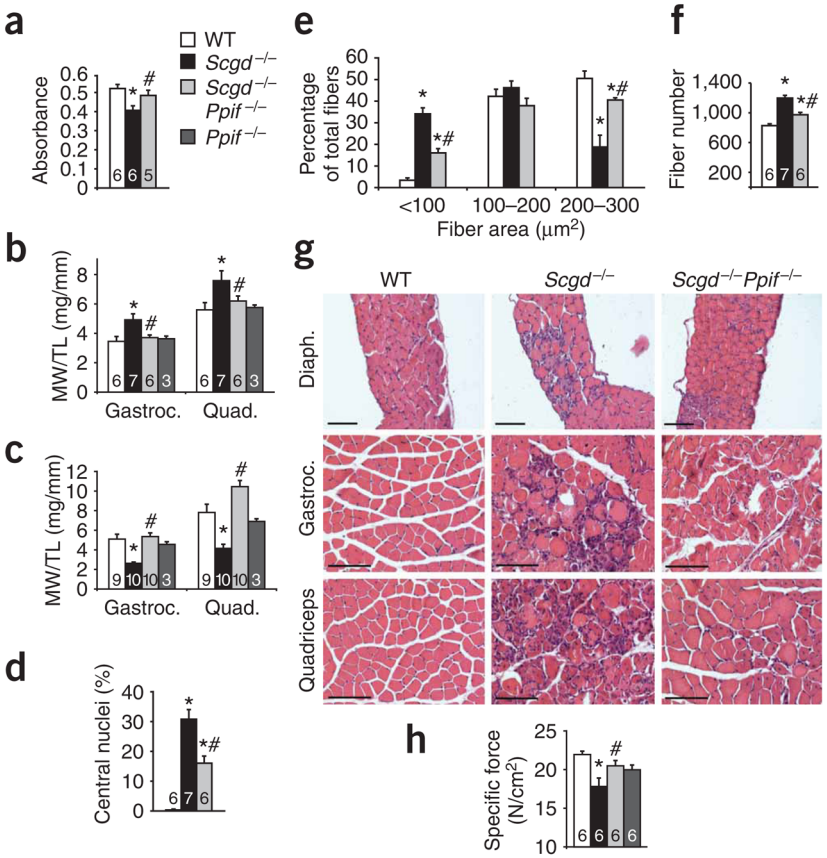

Figure 1.

Loss of cyclophilin D reduces pathology in *Scgd*$^{-/-}$ muscle. (**a**) Mitochondrial swelling, as assessed by light scattering at 540 nm, of mitochondria isolated from muscle of 6-week-old wild-type (WT), *Scgd*$^{-/-}$, and *Scgd*$^{-/-}$*Ppif*$^{-/-}$ mice. (**b**) Muscle weight/tibia length ratio (MW/TL) measurements for gastrocnemius (Gastroc.) and quadriceps (Quad.) of WT (4 males, 2 females), *Scgd*$^{-/-}$ (7 males), *Scgd*$^{-/-}$*Ppif*$^{-/-}$ (6 males) and *Ppif*$^{-/-}$ (1 male, 2 females) mice at 6 weeks of age. (**c**) MW/TL measurements for gastrocnemius and quadriceps of WT (5 males, 4 females), *Scgd*$^{-/-}$ (5 males, 5 females), *Scgd*$^{-/-}$*Ppif*$^{-/-}$ (5 males, 5 females) and *Ppif*$^{-/-}$ (1 male, 2 females) mice at 8 months of age. (**d**) Percentage of fibers containing central nuclei in the gastrocnemius of 6-week-old WT, *Scgd*$^{-/-}$, and *Scgd*$^{-/-}$*Ppif*$^{-/-}$ mice. (**e**) Fiber areas (grouped into size ranges) from diaphragms of 6-week-old WT (4 males, 2 females), *Scgd*$^{-/-}$ (7 males) and *Scgd*$^{-/-}$*Ppif*$^{-/-}$ (6 males) mice. (**f**) Fiber numbers in the gastrocnemius muscle of WT, *Scgd*$^{-/-}$, and *Scgd*$^{-/-}$*Ppif*$^{-/-}$ mice. (**g**) Representative H&E-stained histology of the indicated muscles from the indicated cohorts of mice at 6 weeks of age. Diaph., diaphragm. Scale bars, 100 μm. (**h**) Specific force of isolated EDL muscles from 6 male mice in each group (11 or 12 muscles analyzed in total per group) to assess muscle strength. *P < 0.05 versus WT; #P < 0.05 versus *Scgd*$^{-/-}$. The key in **a** applies to all panels. The sample number for each group is indicated inside each bar. Error bars represent s.e.m.

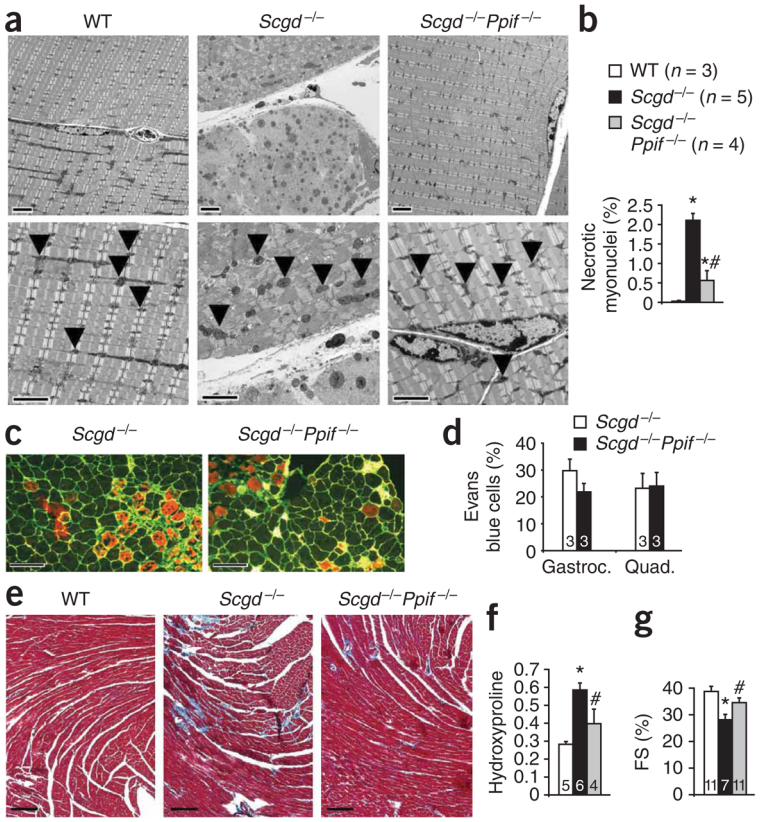

Figure 2.

Analysis of skeletal membrane fragility, ultrastructural defects and cardiac defects. (**a**) Electron microscopy was performed on gastrocnemius muscle from 6-week-old WT, *Scgd*$^{-/-}$, and *Scgd*$^{-/-}$*Ppif* $^{-/-}$ mice. The arrowheads show individual mitochondria. Scale bars, 2 μm. (**b**) Quantification of necrotic myocyte nuclei by hairpin probe hybridization in gastrocnemius histological sections from WT, *Scgd*$^{-/-}$ and *Scgd*$^{-/-}$*Ppif* $^{-/-}$ mice. (**c**) Representative histological fluorescent analysis of myofiber membranes (green) and Evan's blue dye (red) uptake in the gastrocnemius of 6-week-old *Scgd*$^{-/-}$ and *Scgd*$^{-/-}$*Ppif* $^{-/-}$ mice. Scale bars, 100 μm. (**d**) Quantification of Evan's blue dye uptake in gastrocnemius and quadriceps muscle from 3 mice in each group after voluntary exercise and expressed as a percentage of fibers. (**e**) Representative Masson's trichrome–stained histological sections of hearts from 8-month-old WT, *Scgd*$^{-/-}$ and *Scgd*$^{-/-}$*Ppif* $^{-/-}$ mice. Scale bars, 100 μm. (**f**) Measurement of hydroxyproline content in hearts from the three genotypes analyzed in **a** expressed as μg hydroxyproline/mg of tissue. Key is shown in **b.** (**g**) Echocardiography-measured fractional shortening (FS) in the groups of mice indicated in the key in panel **b**. **P* < 0.05 versus WT; #*P* < 0.05 versus *Scgd*$^{-/-}$. The sample number for each group is indicated inside each bar. Error bars represent s.e.m.

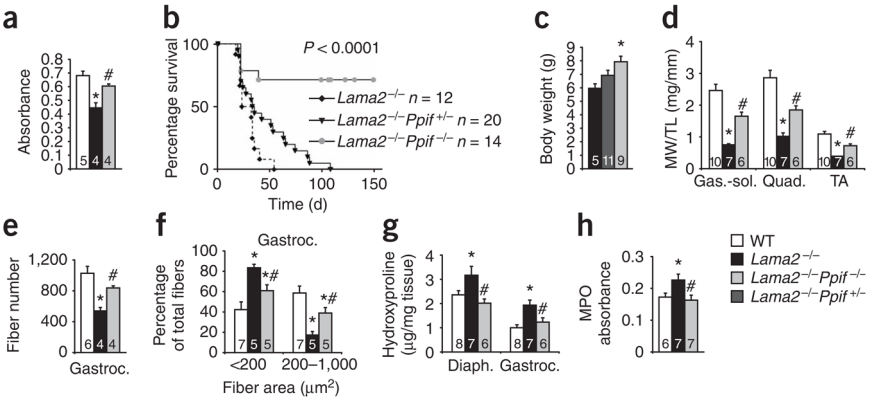

Figure 3.

Genetic ablation of cyclophilin D increases lifespan and reduces muscular dystrophy pathology in *Lama2*$^{-/-}$ mice. (**a**) Mitochondrial swelling, as assessed by light scattering at 540 nm, of mitochondria isolated from skeletal muscle of the indicated groups of mice. The key for all panels is shown in the lower right corner of the figure. (**b**) Survival rate for *Lama2*$^{-/-}$, *Lama2*$^{-/-}$*Ppif* $^{+/-}$ and *Lama2*$^{-/-}$*Ppif* $^{-/-}$ mice. *P* o 0.001 for *Lama2*$^{-/-}$ versus *Lama2*$^{-/-}$*Ppif* $^{-/-}$. (**c**) Body weights of *Lama2*$^{-/-}$, *Lama2*$^{-/-}$*Ppif* $^{+/-}$ and *Lama2*$^{-/-}$*Ppif* $^{-/-}$ mice at 4 weeks of age. WT mice at the same age had an average body weight of 14 g. (**d**) MW/TL for gastrocnemiussoleus (Gas.-sol.), quadriceps (Quad.) and tibialis anterior (TA) from WT (6 males, 4 females), *Lama2*$^{-/-}$ (5 males, 2 female) and *Lama2*$^{-/-}$*Ppif* $^{-/-}$ (4 male, 2 female) mice at 3 weeks of age. (**e**) Fiber numbers in the gastrocnemius muscle of WT (6 male), *Lama2*$^{-/-}$ (4 male) and *Lama2*$^{-/-}$*Ppif* $^{-/-}$ (4 male) mice at 3 weeks of age. (**f**) Fiber areas of gastrocnemius (grouped into 2 size ranges) from 3-week-old WT, *Lama2*$^{-/-}$ and *Lama2*$^{-/-}$*Ppif* $^{-/-}$ mice. (**g**) Hydroxyproline content from diaphragm and gastrocnemius of 3-week-old WT, *Lama2*$^{-/-}$ and *Lama2*$^{-/-}$*Ppif* $^{-/-}$ mice. (**h**) Myeloperoxidase (MPO) activity from quadriceps of 3-week-old WT, *Lama2*$^{-/-}$ and *Lama2*$^{-/-}$*Ppif* $^{-/-}$ mice. **P* o 0.05 versus WT; #*P* o 0.05 versus *Lama2*$^{-/-}$. The sample number for each group is indicated inside each bar. Error bars represents s.e.m.

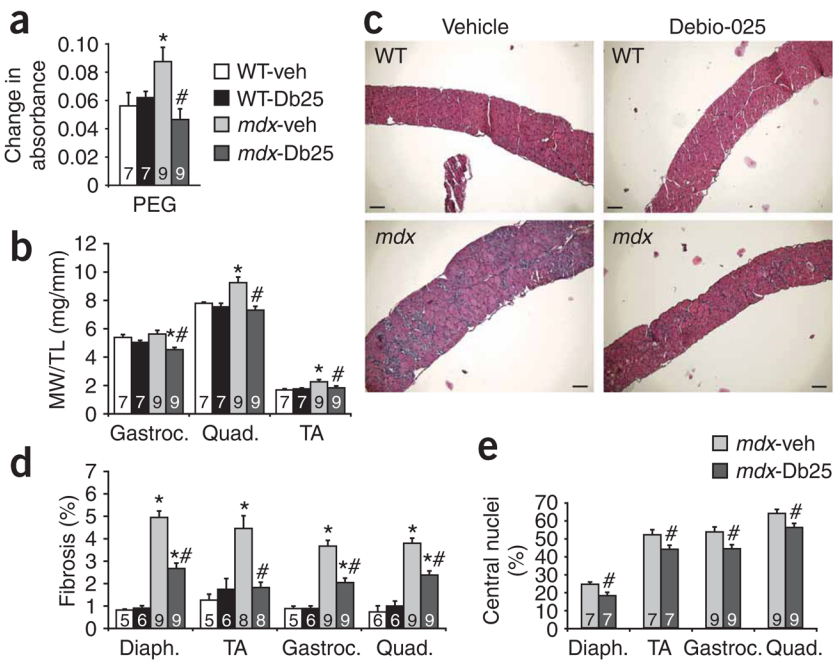

Figure 4.

Debio-025 reduces disease progression in *mdx* mice. (**a**) Changes in mitochondrial absorbance after 10 min of incubation with PEG-3350. The greater the change in absorbance, the greater the mitochondrial shrinkage. Db25, Debio-025. (**b**) MW/TL for gastrocnemius, quadriceps and tibialis anterior of WT and *mdx* mice treated with vehicle or Debio-025. (**c**) Representative histological sections of diaphragm stained with H&E from WT and *mdx* mice treated with vehicle or Debio-025. Scale bars, 100 μm. (**d**) Quantification of fibrotic area from trichrome-stained sections of diaphragm, tibialis anterior, gastrocnemius and quadriceps. (**e**) Percentage of fibers containing central nuclei from diaphragm, tibialis anterior, gastrocnemius and quadriceps. The key in **a** also applies to **b** and **d**. **P* < 0.05 versus WT-veh or WT-Db25; #*P* < 0.05 versus *mdx*-veh. All mice analyzed were male. The sample number for each group is indicated inside each bar. Error bars represents s.e.m.